

Wrya Mohammadi Aframehr<sup>1</sup>

Chaoran Huang<sup>2</sup>

Prof. Peter H. Pfromm<sup>\*1</sup>

## Chemical Looping of Manganese to Synthesize Ammonia at Atmospheric Pressure: Sodium as Promoter

Affordable synthetic ammonia (NH<sub>3</sub>) enables the production of nearly half of the food we eat and is emerging as a renewable energy carrier. Sodium promoted chemical looping NH<sub>3</sub> synthesis at atmospheric pressure using manganese (Mn) is here demonstrated. The looping process may be advantageous when inexpensive renewable hydrogen from electrolysis is available. Avoiding the high pressure of the Haber-Bosch process by chemical looping using earth-abundant materials may reduce capital cost, facilitate intermittent operation, and allow operation in geographic areas where infrastructure is less sophisticated. At this early stage, the data suggest that 0.28 m<sup>3</sup> of a 50% porosity solid Mn bed may suffice to produce 100 kg NH<sub>3</sub> per day by chemical looping, with abundant opportunities for improvement.

### Keywords:

Alkali promoter, Ammonia production, Chemical looping, Manganese nitride, Renewable energy-carrier

### Author affiliations

<sup>1</sup> Washington State University, Voiland School of Chemical Engineering and Bioengineering, 305 NE Spokane St, 99163, U.S.A.

<sup>2</sup> Kansas State University, Tim Taylor Department of Chemical Engineering, 1701A Platt St, 66506, U.S.A.

Email corresponding author: peter.pfromm@wsu.edu

This is the author manuscript accepted for publication and has undergone full peer review but has not been through the copyediting, typesetting, pagination and proofreading process, which may lead to differences between this version and the [Version of Record](#).

Please cite this article as [doi: 10.1002/ceat.202000154](https://doi.org/10.1002/ceat.202000154)

This article is protected by copyright. All rights reserved.

## 1. Introduction

Ammonia ( $\text{NH}_3$ ) made using renewable energy rather than fossil fuels would reduce fossil  $\text{CO}_2$  emissions, and would contribute to decoupling our food from fossil fuels [1] through providing renewable fertilizers. Additionally, hydrogen ( $\text{H}_2$ ) in the form of  $\text{NH}_3$  is emerging as a potential vector for renewable energy [2] due to some advantages over  $\text{H}_2$  [3] despite the energy penalty of converting  $\text{H}_2$  to  $\text{NH}_3$ . Renewable hydro electricity-based  $\text{NH}_3$  has long been made at the industrial scale by supplying  $\text{H}_2$  from water electrolysis to the Haber-Bosch (H.-B.) process [4] in at least five locations [5] due to locally available inexpensive hydroelectricity (among them Sable Chemicals, Kwekwe, Zimbabwe; KIMA, Aswan Dam, Egypt; and Industrias Cachimayo, Cuzco, Peru). Renewable (excess) electricity from wind turbines, solar photovoltaic systems, or hydropower is often intermittent at time scales of hours, days, or months [6]. The H.-B. process, however, is not easily started up or shut down. H.-B. economics become less favorable when scaled down [7] from the typical world-scale production rates of a kiloton  $\text{NH}_3$  or more per day. The H.-B. process is technically and operationally challenging due to the turbocompressor technology [8] to reach operating pressures of 200 atmospheres or more, along with strict requirements to protect H.-B. catalysts from oxygen. There is no economic or technological rationale to replace the H.-B. process for production at the world-scale, with  $\text{H}_2$  derived either from fossil fuel through steam reforming, or from renewable energy by electrolysis [1]. However, ton per day rather than kiloton per day scale, rugged intermittent operation, and process simplification may perhaps be desirable and might be achieved by approaches such as chemical looping investigated here [9,10] instead of the H.-B. process. The work presented here advances towards a workable chemical looping process using metal nitrides to produce  $\text{NH}_3$  from renewable  $\text{H}_2$ , and dinitrogen ( $\text{N}_2$ ) derived from the air.

Chemical looping with nitrides is one approach to activation of the dinitrogen molecule for a chemical reaction [11] somewhat similar to the perhaps more familiar chemical looping using oxides [12]. Manganese (Mn) is the metal selected here based on previous work [13] as the carrier to supply activated (atomic) nitrogen (N) in the form of Mn nitrides to a second step where  $\text{NH}_3$  is formed. The N-depleted solid is then recycled and "loaded" again with N atoms to close the loop (Fig. 1). It should be noted that in the process investigated here, different gases are directed over a stationary bed of solid particles, while in more conventional chemical looping with oxides, the solid particles are generally moved from one

reactor to another. Moving large amounts of solid particles is generally challenging, and this is here avoided in the proposed looping of Mn to synthesize  $\text{NH}_3$ .

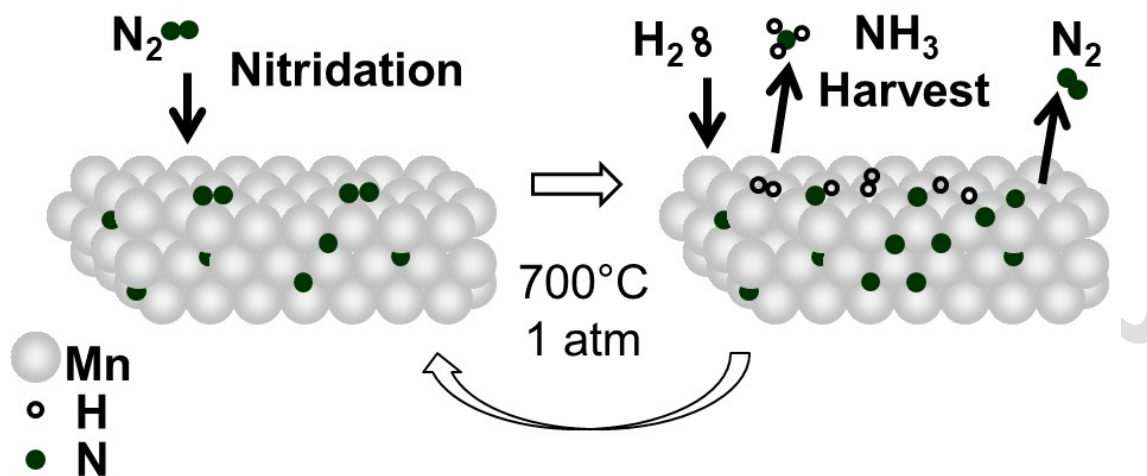


**Figure 1.** Principle of chemical looping  $\text{NH}_3$  synthesis from  $\text{H}_2$  and  $\text{N}_2$  at atmospheric pressure and elevated temperature. Mn nitrides are used as N carriers. Parasitic  $\text{N}_2$  formation during  $\text{NH}_3$  harvest lowers the yield (right side). Incomplete N removal during harvest creates a dead load. (Atomic diameters roughly to scale; a simplified Mn lattice is shown).

The chemical looping process differs significantly from the familiar heterogeneous catalytic (H.-B. type)  $\text{NH}_3$  synthesis process. In chemical looping, nitrogen *atoms* are supplied stored as a bulk metal nitride are supplied to the surface of the solid particles, while hydrogen molecules are provided via the gas phase. This may allow overcoming the well-known tradeoffs of heterogeneous H.-B. catalysts since dinitrogen activation and  $\text{NH}_3$  synthesis are decoupled in time.  $\text{NH}_3$  must be formed at the solid/gas interface where lattice N atoms and  $\text{H}_2$  from the gas phase meet since severe kinetic limitations would prevent  $\text{NH}_3$  formation in the gas phase in case lattice N atoms emerge and potentially recombine to  $\text{N}_2$ .

Summarizing, the overall approach is then to first convert Mn to Mn nitrides by contacting a fixed bed of Mn particles (with or without a promoter added) with  $\text{N}_2$  at atmospheric pressure and about  $700^\circ\text{C}$  to activate the dinitrogen by bulk Mn nitride formation. In a second step,  $\text{NH}_3$  is harvested by directing a stream of  $\text{H}_2$  over the Mn nitride bed. Synthesis of  $\text{NH}_3$  at atmospheric pressure and elevated temperature by chemical looping of Mn is compared here to the same chemical looping but with some sodium hydroxide (NaOH) added to promote  $\text{NH}_3$  formation [14]. Looping was repeated for a total of three  $\text{NH}_3$

harvest cycles (Fig. 2), both with analysis of the solid between the steps of looping and in a continuous mode simulating operation in a technical setting.

The overall goal of the work is to show reproducibility for several cycles of a chemical looping  $\text{NH}_3$  synthesis process operating near-atmospheric pressure to avoid the cumbersome high pressure of the H.-B. synthesis and facilitate scale-down and intermittent operation. This is attempted by decoupling the  $\text{N}_2$  activation step from  $\text{NH}_3$  synthesis through the chemical looping of Mn. It is shown here how a sodium-containing promoter facilitates Mn chemical looping  $\text{NH}_3$  synthesis. It is encouraging that repeated looping of Mn or Mn with the promoter shows no deterioration of the performance as far as  $\text{NH}_3$  yield and kinetics.

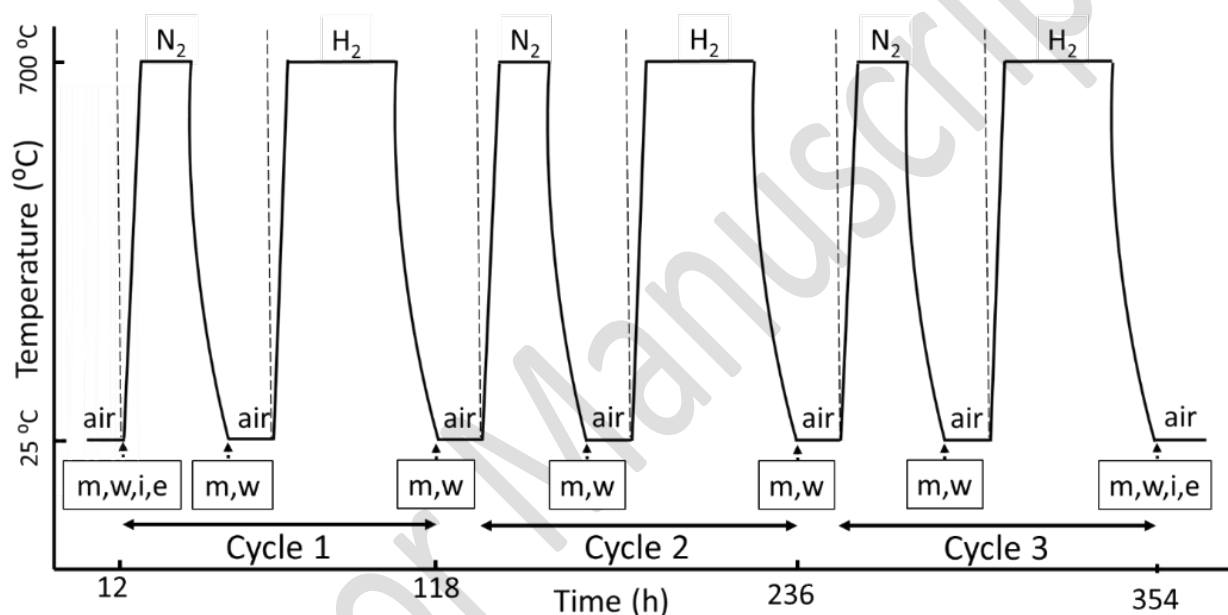


**Figure 2.** Overall process and parameters of chemical looping tests in "stop mode" reported here. m, w, i, and e indicate weighing, WAXD, I.C.P., and S.E.M., respectively. "air" indicates that the cooled sample was removed from the furnace, manually ground with mortar and pestle, and returned to the furnace.

## 2. Materials and Methods

### 2.1. Materials

Manganese metal (Mn) and Mn(II) oxide ( $\text{MnO}$ ) were obtained as particles from Alfa Aesar (No. 45089, average particle size <10 micrometers, 99.6% pure, and No. 44441, 99.99% pure, respectively; Fig. 3). Sodium Hydroxide ( $\text{NaOH}$ ) pellets were from Fisher Chemical (No. S318, certified A.C.S., >95% pure). Ammonium hydroxide ( $\text{NH}_4\text{OH}$ ) stock solution was purchased from LabChem, Inc. (50% v/v (1+1), 13.04 wt%  $\text{NH}_4\text{OH}$ , No. LC111404) for

calibration of the colorimetric ammonia test kit (API<sup>®</sup> Ammonia Test Kit, No. B000255NC8). Compressed H<sub>2</sub> and dinitrogen (N<sub>2</sub>, ultra-high purity) were supplied by A-L Compressed Gases Inc., Spokane. Gas-phase NH<sub>3</sub> concentration was measured using Dräger tubes (Drägerwerk AG & Co. KGaA, Germany, Dräger Accuro pump kit No. 4053473, tubes No. 8101941 for 2.5–100 ppm and No. CH20501 for 5–700 ppm of NH<sub>3</sub>, estimated error ±10% of the measured value) Alumina combustion boats (Coorstek Inc. No. 65568) were used. Quartz tubes for the tube furnace (inner diameter 45 millimeters, Technical Glass Products Inc., No. 45X48) were customized via glass blowing by narrowing on the inlet side to attach the gas feed and provided with custom end caps. All gas handling manifolds were constructed from Swagelok stainless steel fittings and tubing (1/8 inch, Swagelok, S. Kent, Washington). Cooled gas downstream of the tube furnace was routed via polymer tubing (1/4 inch, Watts, Andover, MA, SVGE20). Deionized water was used for the absorption of NH<sub>3</sub> from the cooled gas exiting the furnace tube. A bubble diffusor (Bubbling Airstone, Imagitarium) was used to disperse the gas from the reactor in a water column held in a graduated cylinder (1 liter, Thermo Scientific, Austin, TX, 3662-1000, ±6 milliliter limit of error). A second identical cylinder in series was used to confirm complete NH<sub>3</sub> recovery.

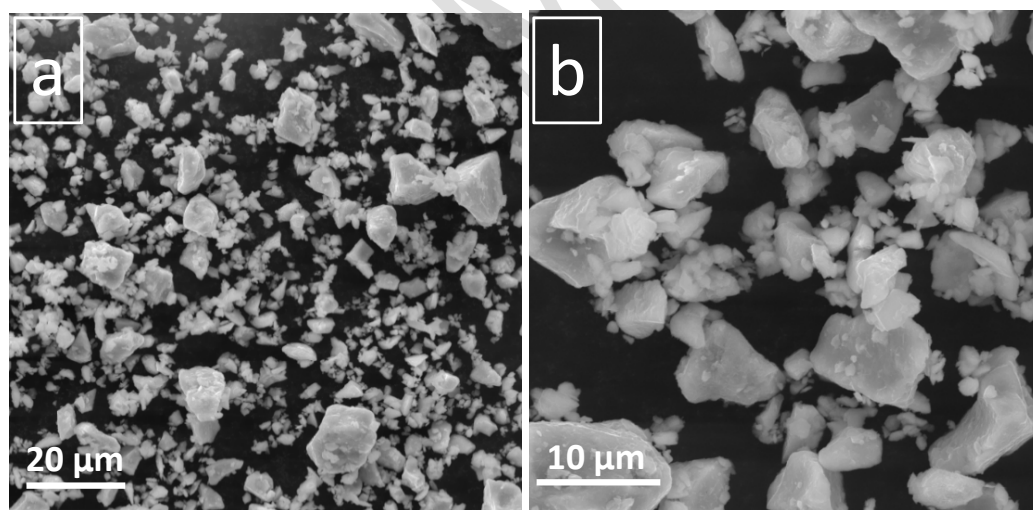


**Figure 3.** Scanning electron micrograph of as-received Mn particles. The size distribution is significant with a population of larger particles (on the order of 10 μm), and a population with a much smaller size (on the order of 1–8 μm).

## 2.2. Methods

### 2.2.1. Ammonia analysis

The gas from the furnace was cooled and then directed through two graduated cylinders with bubble diffusers in series (see Fig. 4) where  $\text{NH}_3$  is absorbed in the water at room temperature.  $\text{NH}_3$  is then detected via colorimetry in appropriately diluted samples from both cylinders, confirming that the  $\text{NH}_3$  in the second cylinder was non-detect. Concentrations detected by colorimetry in a typical experiment were in the range of 0.5-4 ppm. The combined error of dilution and colorimetry is estimated at  $\pm 0.02$  ppm from 0.25 to 0.5 ppm  $\text{NH}_3$ ,  $\pm 0.04$  ppm from 0.5 to 1 ppm,  $\pm 0.15$  ppm from 1 to 2 ppm, and  $\pm 0.20$  ppm from 2 to 4 ppm. The cumulative amount of  $\text{NH}_3$  synthesized was then calculated by multiplying the detected  $\text{NH}_3$  concentration with the graduated cylinder liquid volume at the time and adding the previous amounts of recovered  $\text{NH}_3$  (Fig. 5, Figs. 1s and 2s (see supporting information)). Error bars indicated in Figs. 5, 1s, and 2s represent the cumulative errors of all individual colorimetric measurements.

pH was monitored (pH meter Accumet XL150, Fisher Scientific, New Hampshire, U.S.A.). Occasionally gas was sampled and analyzed using Dräger tubes following the Manufacturer's instructions. This was to verify that negligible amounts of  $\text{NH}_3$  escaped the absorption system.

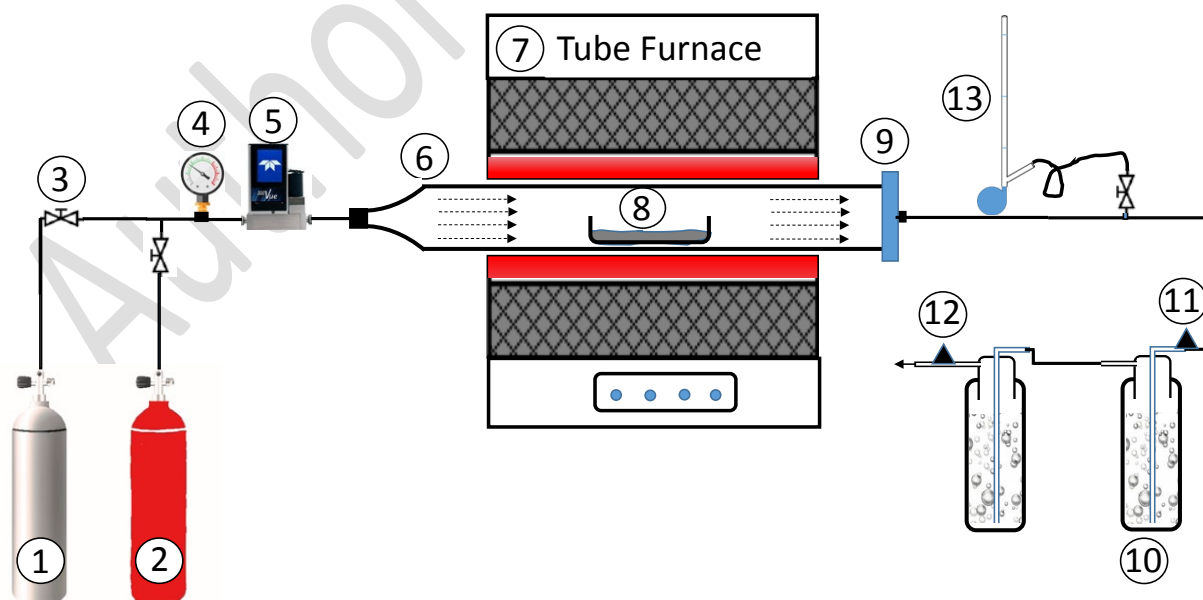


**Figure 4.** System for chemical looping. (1)  $\text{N}_2$  cylinder, (2)  $\text{H}_2$  cylinder, (3) metering valve, (4) pressure gauge, (5) mass flow controller, (6) fused quartz furnace tube, (7) electric tube furnace, (8) alumina combustion boat with a solid

reactant, (9) tube end cap, (10) gas washbottle, (11), (12) Dräger NH<sub>3</sub> gas detection tube sampling, and (13) bubble flowmeter.

### **2.2.2. Characterization of solids: imaging, wide angle X-ray diffraction (WAXD), inductively coupled plasma spectroscopy (I.C.P.), X-ray photoelectron spectroscopy (XPS)**

Particle morphology and qualitative surface composition were examined via scanning electron microscopy (S.E.M.) with energy-dispersive X-ray spectroscopy (E.D.S.) (Tescan Vega3, Team E.D.S. system, Ametek Edax, Middleboro, MA). Transmission electron microscopy (T.E.M.), (Tecnai T20, Thermo Scientific-FEI, Waltham, MA, U.S.A.) specimens were prepared by dispersing particles in ethanol and drop-casting on the surface of formvar/carbon-coated nickel meshes (Electron Microscopy Sciences, Inc., FCF200-Ni) followed by drying in a vacuum desiccator for 24 hours.

Wide angle X-ray diffraction (WAXD) patterns were recorded on a Rigaku Miniflex 600 (Rigaku, Japan) with Cu K $\alpha$  radiation ( $\lambda = 1.54 \text{ \AA}$ ), 40 kV/15 mA output and diffracted beam monochromator, between 20 and 100° 2 $\theta$  (1° 2 $\theta$ /min scan speed, 0.02 data points/°2 $\theta$ , continuous mode). WAXD samples were prepared by manual compaction into Si standard sample holders. The International Centre for Diffraction Data (ICDD) PDF-2 database was used for phase identification. All solid samples were stored in glass vials under N<sub>2</sub> at room temperature and atmospheric pressure when not in use.

The ICP-MS (Agilent 7500cx, Agilent Technologies Inc., Santa Clara, U.S.A.) samples were prepared and analyzed as described elsewhere [15]. About 20 milligrams solid was dispersed in 3 milliliters (ml) of concentrated nitric acid (HNO<sub>3</sub>, 69–70%) and 2 ml of 30% H<sub>2</sub>O<sub>2</sub>, and then heated to 120 °C in a block digester for 1 hr. 1 ml of internal standard solution was added (10 micrograms per ml, Bi, Li-6, Sc, Tb, and Y; Accustandard, Inc., New Haven, CT, U.S.A.) to each digested solution and diluted to 100 ml using deionized water before analysis.

X-ray photoelectron spectroscopy (XPS) was performed using a Perkin Elmer PHI 5400 (Physical Electronics, Inc., Chanhassen, MN, U.S.A., monochromatic Al K radiation, 1486.6 eV, 20mA, 15kV). The Base pressure of the analysis chamber during measurement was less than 1.3 10<sup>-8</sup> torr. Calibration was by setting the binding energy of Au<sub>4f7/2</sub> and Cu<sub>2p3/2</sub> to 84.0 and 284.6 eV, respectively, with pass energy 17.9 eV. The analyzer pass energy was set to 44.75 eV and contact time 100 ms. For high resolution measurement of Mn<sub>2p3/2</sub>, Mn<sub>3s</sub>,

C<sub>1s</sub>, and O<sub>1s</sub>, pass energy was set to 17.9 eV and contact time 25 ms. Ar ion gun sputter was used to clean the sample surface. The charge correction was using the binding energy of C<sub>1s</sub> 284.8 eV as a reference. Spectra were analyzed by using CasaXPS (Casa Software Ltd.) with Shirley background. Gaussian-Lorentzian (50:50) contribution was used for the best fit.

### 2.2.3. Tube furnace procedures, chemical looping

The chemical looping procedure (nitridation of Mn/NH<sub>3</sub> harvest) was carried out in two modes: (i) analyzing the solid between cycles, requiring cool down, opening of the tube furnace, and re-heat (dubbed "stop mode") and (ii) continuous cycling without cool down or other interruptions to simulate actual looping operation (dubbed "non-stop mode"). An overview of the chemical looping procedure of the stop mode is shown in Fig. 2. Overall, solids were loaded into a ceramic boat and placed in the center of the furnace tube, gases were then directed through the tube, and heat up/holding/cool down (stop mode) was executed, with analytical procedures between cycles as indicated in Fig. 2. About 5 grams of Mn and 5 grams of Mn with 0.25 grams NaOH promoter added was loaded initially into the combustion boat. Weight and WAXD spectra were obtained every time the sample was cooled, with more extensive analysis before and after all cycling was completed. No solids were added or removed during the three cycles. To simulate actual operation, the stop mode experiments were then repeated without interruption (non-stop mode) by simply successively directing N<sub>2</sub> (nitridation) and H<sub>2</sub> (NH<sub>3</sub> harvest) over the solid bed for three cycles.

#### 2.2.3.1. Temperature control:

A tube furnace (Thermo Scientific Lindberg/Blue M, No. STF54434C) was used. The temperature as set at the furnace controller exceeded the actual temperature in the sample boat by at maximum 17 ° C as determined using a thermocouple (Omega/C L 3515R). A furnace heats up followed the linear relationship in Eq.1 below while cooling after power off followed Eq. 2.

$$T=63.86t+59.03 \quad (1)$$

$$T=698.58 e^{(-0.016t)} \quad (2)$$

where T (° C) and t (min) are furnace controller setpoint temperature and time, respectively. A Mass Flow Controller (Teledyne Hastings Instruments HFC-D-302B(H), Teledyne



Hastings, Hampton, VA, U.S.A.) was used to control gas flow, occasionally verified using a bubble flowmeter (Fig. 4).

#### 2.2.3.2. Initial preparation of the solid:

Mn was used as received. If NaOH (as received) was added to Mn, then the solids were mixed manually by mortar and pestle for about 10 minutes. About 5 grams of Mn, with about 0.25 grams of NaOH added for the promoter experiments was then loaded in a combustion boat.

#### 2.2.3.3. Nitridation, NH<sub>3</sub> harvest:

The purging procedure described here was performed after every interruption in the stop mode, and before starting the non-stop mode experiments. After loading solids and before placing the boat in the tube furnace, the boat was always dried in a separate oven at 100°C for about 60 minutes in the air. The loaded boat was then placed in the furnace and N<sub>2</sub> or H<sub>2</sub>, respectively, was directed over the sample at about 100°C for about 60 minutes. The sample was then purged with the respective gas at room temperature before heatup to process temperature. All pre-process purging in the furnace tube was at a gas flow of 1.3 cm<sup>3</sup><sub>(S.T.P.)</sub>/s. When heatup was initiated for stop mode experiments, the gas flow rate was set to 10±0.5 cm<sup>3</sup><sub>(S.T.P.)</sub>/s for nitridation, or 2.6±0.5 cm<sup>3</sup><sub>(S.T.P.)</sub>/s H<sub>2</sub> for NH<sub>3</sub> harvest. Holding time for reaction, and cooldown (power off to the furnace) were then performed (Fig. 2). After each cooldown the solids were re-ground by mortar and pestle, and either replaced in the boat for the next cycle (above), or further analyzed after the final cycle (I.C.P., WAXD, microscopy, XPS). In non-stop mode, the gas flow rate was set to 10±0.5 cm<sup>3</sup><sub>(S.T.P.)</sub>/s for nitridation, or 2.6±0.5 cm<sup>3</sup><sub>(S.T.P.)</sub>/s H<sub>2</sub> for NH<sub>3</sub> harvest.

In both stop mode and non-stop mode when H<sub>2</sub> was used for the NH<sub>3</sub> harvest, the gas from the reactor was cooled by flow through about 4 meters of vinyl tubing at room temperature and sent to the NH<sub>3</sub> absorption system for periodical analysis by colorimetry, and sometimes verification using Dräger tubes. All solids were weighed (Mettler Toledo, No. MS204S/03, ±0.00005 grams).

### 3. Results and Discussion

The goal of the experiments reported here was to show that successive chemical looping of Mn shows no significant deterioration in  $\text{NH}_3$  synthesis as far as yield and rate of conversion. Both an analytical experimentation mode ("stop mode") with solids analysis between chemical looping steps, and a "non-stop mode" as would be performed in a realistic process were performed, with similar results. A scale-up estimate is also attempted.

The following experiments were carried out for reference and are not reported in detail here for brevity, all at atmospheric pressure: (a) directing  $2.6 \text{ cm}^3_{(\text{S.T.P.})}/\text{s}$   $\text{H}_2$  at  $700^\circ\text{C}$  over as-received Mn particles in a combustion boat (b) directing  $2.6 \text{ cm}^3_{(\text{S.T.P.})}/\text{s}$   $\text{H}_2$  at  $700^\circ\text{C}$  over an empty combustion boat (c)  $\text{N}_2$  followed by  $\text{H}_2$ , both at  $700^\circ\text{C}$  over pure  $\text{MnO}$ . No  $\text{NH}_3$  was detected in any of the tests above.

#### 3.1. Looping is successful for three $\text{NH}_3$ harvest cycles, Na promoter accelerates the process, and increases yield

Fig. 5 shows the cumulative amount of  $\text{NH}_3$  harvested from the first cycle of chemical looping of as-received Mn particles, and for the Mn particles with NaOH added as a promoter in both stop mode and non-stop mode (see Figs. 1s and 2s available in supporting information for two additional cycles, data is essentially identical to Fig. 5). The increased yield and accelerated evolution of  $\text{NH}_3$  using the promoter are significant in both stop and non-stop modes. Notably, the effect of the promoter does not subside over three nitridation/harvest cycles.

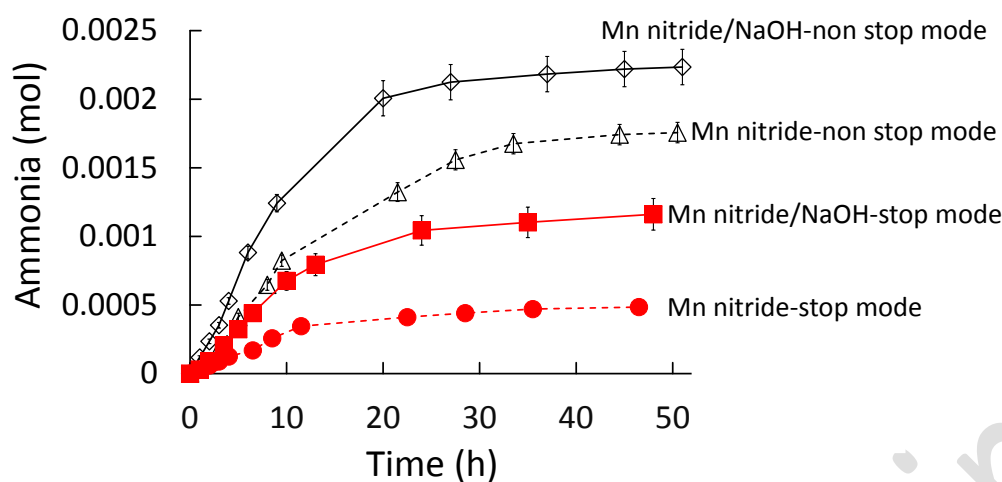


**Figure 5.** Ammonia harvest from the first chemical looping cycle of about 5 grams of Mn, and 5 grams Mn with 0.25 grams NaOH promoter added in both stop mode (solid symbols) and non-stop mode (open symbols). Two subsequent nitridation/harvest cycles were performed but are essentially identical and omitted here (see supporting information for all three looping cycles of Mn and Mn with promoter). The addition of Na promoter and non-stop mode significantly improves yield and cycle time.

The promoter is hypothesized to improve the conversion of N atoms emerging from the solid nitride since it appears unlikely that diffusion of N in the solid material or any gas phase processes could be altered by the presence of the promoter. Adding NaOH to Mn may lead to mass transfer and/or thermodynamics favoring the release of N atoms to the surface for ammonia synthesis. However, one is left at this point with hypothesizing based on limited circumstantial evidence.

The similarity of a side-by-side comparison of the WAXD spectra (Fig. 6) with and without promoter after the first nitridation and after the last harvesting indicates any possible promoter effect that could be detected by WAXD.

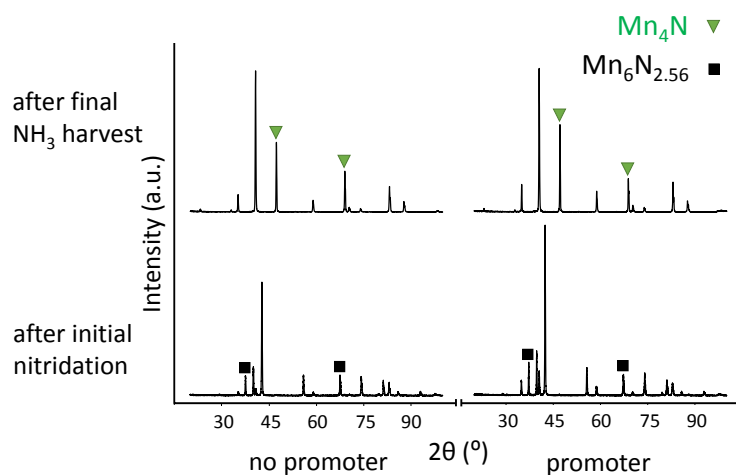


**Figure 6.** Side-by-side comparison for WAXD spectra of the solid after initial nitridation and after final  $\text{NH}_3$  harvest during chemical looping with and without NaOH promoter. The similarity of the spectra and their expected change upon nitridation (prominent nitride peaks indicated by solid square, and triangle:  $\text{Mn}_2\text{N}_{0.86}$  (PDF number: 01-077-2007) and  $\text{Mn}_4\text{N}$  (PDF number: 01-089-7380), respectively) supports the notion that the promoter does not impact the bulk of the solid, but modifies the conversion of N with  $\text{H}_2$  to  $\text{NH}_3$  at the solid surface (additional peak assignments can be found in the on-line materials).

### 3.2. Composition of Mn particles

WAXD of as-received Mn particles shows the expected spectrum for metallic  $\alpha$ -Mn (Fig. 7). The  $\alpha$ -Mn unit cell containing 51 atoms is quite complex and has notably been described as "exotic" [16]. Also, the nitridation of manganese results in several different phases (Fig. 7). These phases can convert over time driven by thermodynamics. Phase changes are therefore seen with the nitrogen deadload and the intrusion/removal of nitrogen during looping.

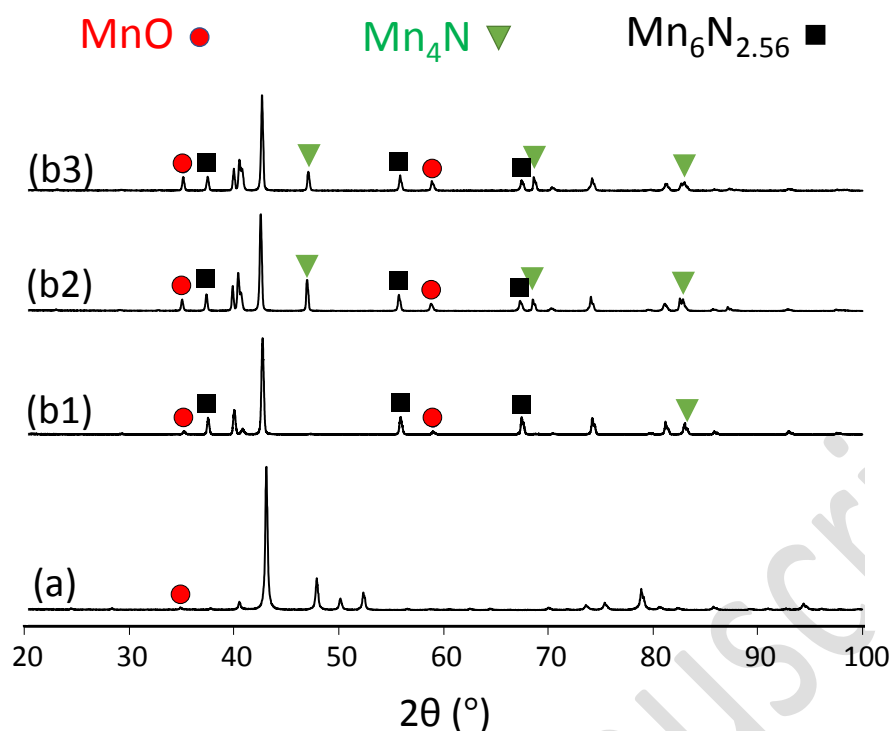


**Figure 7.** Wide-angle x-ray diffraction patterns of (a) as received Mn, (b1),(b2) and (b3) Mn after first, second, and third nitridation, respectively. Solid circle, square, and triangle: MnO (Powder Diffraction File (PDF) number: 01-077-2929),  $\text{Mn}_2\text{N}_{0.86}$  (PDF number: 01-077-2007) and  $\text{Mn}_4\text{N}$  (PDF number: 01-089-7380), respectively (additional peak assignments can be found in the on-line materials).

The surface of the as-received Mn particles shows oxides as detected by XPS. Fig. 8 shows three multisplitting peaks for  $\text{Mn}_{2p_{3/2}}$  spectra at 640.6, 641.9, and 646.6 eV assigned to MnO ( $\text{Mn}^{2+}$ ),  $\text{Mn}_2\text{O}_3$  ( $\text{Mn}^{3+}$ ), and MnO ( $\text{Mn}^{2+}$ ) satellite, respectively. The relative amounts of MnO ( $\text{Mn}^{2+}$ ) and  $\text{Mn}_2\text{O}_3$  ( $\text{Mn}^{3+}$ ) are estimated at 30 atom% and 70 atom%, respectively. Mn metal ( $\text{Mn}^0$ , 638.6 eV) is below detection limits. The dominance of Mn oxides is not unexpected, and any technical scale process will very likely be performed with some surface oxidation of the metal particles since the complete exclusion of oxygen would require heroic measures.

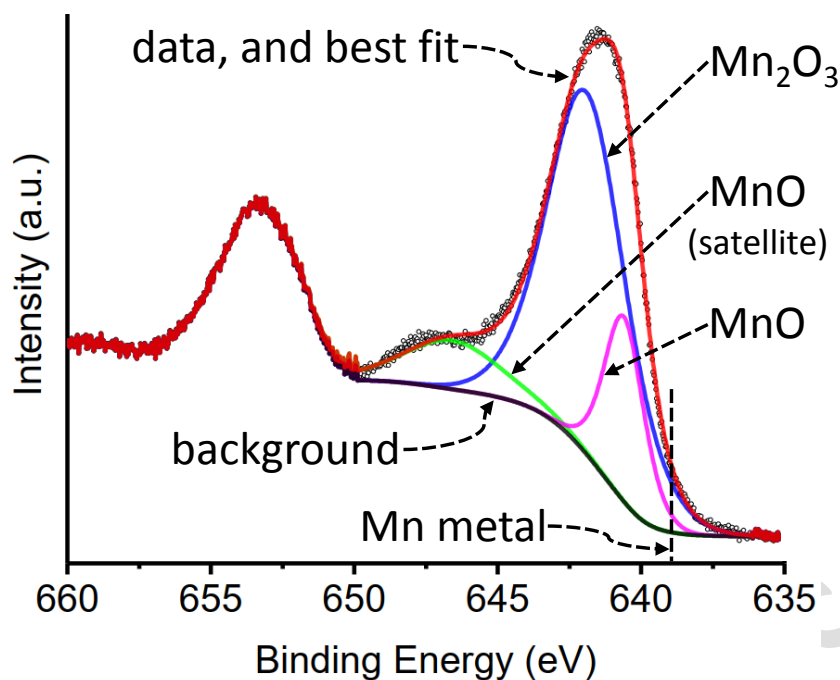


**Figure 8.** XPS Mn<sub>2p<sub>3/2</sub></sub> spectra for as-received Mn particles. The surface appears to contain only oxides, and metallic Mn is considered below the detection limit.

In the stop mode experiments, the WAXD spectra of the solid taken before chemical looping, and after each nitridation step (Fig. 7) indicates increasing but leveling-off Mn oxide content. It is apparent from the reproducible chemical looping that the presence of Mn oxide up to about 3 atom% does not impede the chemical looping. Mn oxides are known to interact with activated N donated from certain chemicals by forming oxynitrides that are of interest as catalysts [17]. However, it may not be possible to detect this with the techniques used here due to the relatively small mass and thickness of the oxide "skin" of the particles. By adding the NaOH as a promoter, oxygen will be added to the system too, our research shows that having the oxygen could effect on productivity. So adding more NaOH is not enhancing NH<sub>3</sub> production necessarily.

There are several nitride phases formed during nitridation of Mn in nitrogen at elevated temperature [18]. The absolute and relative amounts of these phases depend on temperature and time at temperature. The Mn<sub>6</sub>N<sub>2.58</sub> with a higher amount of N is the most advantageous phase for subsequent thermochemical looping NH<sub>3</sub> synthesis due to changes in stability and mass transfer of N in this phase. The conditions here were chosen based on previous work cited above to maximize the amount of nitrogen absorbed by the Mn. The Mn

nitride phases after each nitridation during repeated looping are identified in WAXD spectra in the supporting information.

### 3.3. Mn interaction with promoter NaOH

The relatively low melting point of the NaOH promoter (M.P. 318.4°C, [19]) indicates that the Mn particles are exposed to molten NaOH, at least on first heating of the Mn/promoter mixture. Any metallic Mn exposed to NaOH will oxidize to MnO, releasing H<sub>2</sub>, and producing solid Na<sub>2</sub>O [22] (M.P. 1132°C). The amount of NaOH added in the promoter experiments would allow for a maximum of about 3 atom% of the Mn to be oxidized to MnO if all NaOH is fully converted to Na<sub>2</sub>O and the released O is completely retained as MnO. In conclusion, after the first looping cycle, the Mn particles with added promoter will likely present a surface layer of oxidized Mn, even if the surface was not completely oxidized initially. MnO content in further cycles levels off, supported by unchanged performance in a second and third cycle.

Based on ICP-MS analysis, the Na content after the third and final chemical looping cycle was 2.28 ±0.29 mg/g or 0.25wt%Na compared to a hypothetical content of 4.80 wt% Na if all Na that was added initially was still present. While some NaOH may well evaporate after melting, the I.C.P. analysis of the final solid and the persistent effect during chemical looping indicate that some Na remains. Whether this is as more refractory NaO, or as adsorbed NaOH with a much reduced vapor pressure compared to bulk NaOH remains to be investigated.

Na, Mn, and O may form other complex compounds on the surface of the particles [20,21]. This may not be detectable by WAXD due to the likely small amounts. This is an additional mechanism to retain Na in the solid, besides physical adsorption.

In summary, while some reactions occur during initial heating of an Mn/NaOH mixture, Na remains with the solid after three chemical looping cycles, and the reproducibility of successive reproducible looping indicates resilient performance by the Mn/promoter mixture.

### 3.4. Yield

The maximum theoretical NH<sub>3</sub> yield based on about 5 grams of Mn nitride containing about 8 wt% of N is 28 millimol NH<sub>3</sub>. This assumes that every N atom is recovered from Mn nitride, and converted to NH<sub>3</sub>. The best yield achieved here experimentally using about 5 grams of Mn is about 1.3 and 2.2 millimol NH<sub>3</sub> in the stop mode and non-stop mode,

**This article is protected by copyright. All rights reserved.**

respectively. The yield reduction is due to unconverted N remaining in the Mn, and likely parasitic formation of  $N_2$  rather than the desired  $NH_3$ .

Fig. 9 shows that some Mn nitride remains after the  $NH_3$  harvest. Assuming that other processes impacting sample mass (vaporizing materials, residual oxidation of Mn) are negligible at least for the third looping cycle, the mass loss between the last nitridation and the last  $NH_3$  harvest is 79.6 mg equivalent to 5.68 mmol N. Since about 1.3 and 2.2 mmol  $NH_3$  was actually harvested, a yield of about 23 and 39 atom% can be assigned for the "active" (removable from the solid over the experimental time frame) N for the stop mode and non-stop mode, respectively. The deadlock of unconverted nitride and the cycle time could likely be improved by using smaller particles (or removing the large particle fraction from the sample, see Fig. 3) to tackle the issue of N diffusion in the solid.

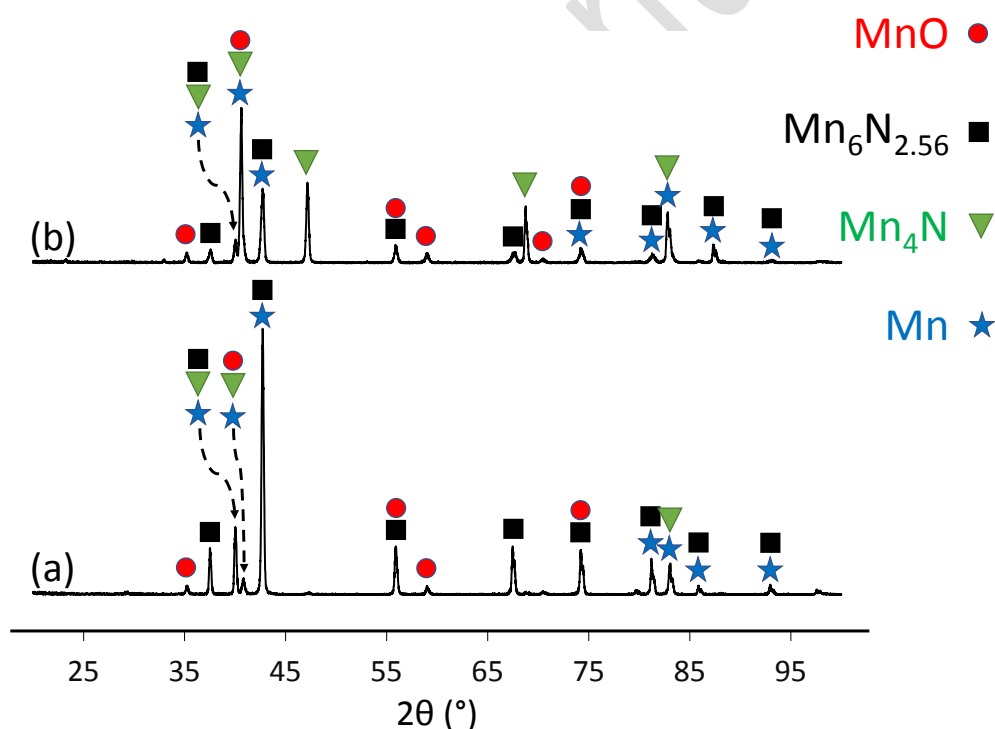


**Figure 9.** WAXD spectra of Mn nitride before (a) and after (b)  $NH_3$  harvesting. Some nitride remains after  $NH_3$  harvesting levels off likely due to increasing N diffusion limitations in the solid particles as the outermost nitride is depleted first. Solid circle, square, and triangle: MnO (PDF number: 01-077-2929),  $Mn_2N_{0.86}$  (PDF number: 01-077-2007), and  $Mn_4N$  (PDF number: 01-089-7380), respectively, and also the hollow circle shows Mn (PDF number: 01-089-2412).



Parasitic conversion of N to dinitrogen instead of  $\text{NH}_3$  formation is another likely issue that may reduce the  $\text{NH}_3$  yield. Promoter presence clearly helps with this, and better promoter distribution, for example, by more uniform solution-based promoter impregnation of Mn particles may help here. For the non-stop mode, the yield is higher both for Mn and Mn/NaOH. The increased introduction of oxygen during the process interruptions in stop mode may cause an increased oxide layer in the particle surface, which may in turn impact N transport negatively as shown in Fig. 3s (see supporting information). This is one of the issues that may lead to the slower conversion in the less realistic "analytical" stop mode vs. the "practical applied" non-stop mode that is closer to the actual operation of this looping process.

### 3.5. Morphology

S.E.M. images of as received Mn particles are presented in Fig. 3. Additional images (see supporting information, Figs. 4s and 5s) show the cross-section of the particle agglomerate after initial nitridation and after the final  $\text{NH}_3$  harvest. It appears that some morphological change occurs, as can be seen in a roughening of the surfaces. This does not appear to impede the reproducibility of chemical looping.

Transmission electron microscopy (T.E.M., Fig. 6s, see supporting information) showed a filamentous surface structure (10-15 nm) for as received Mn. This is no longer seen after chemical looping. This filamentous material may well be collapsed onto the particle surface at temperatures used here.

### 3.6. Scale-up estimate

Assuming a yield of 2.2 millimol  $\text{NH}_3$  per 5 gram of Mn (see above), an improved average Mn particle diameter of 2  $\mu\text{m}$ , and dependence of N atom flux at the Mn nitride particle surface proportional to the inverse of the square of the particle radius (shrinking core model), one can estimate the order of magnitude of Mn needed to reach a given daily production of  $\text{NH}_3$ . With the above parameters, an order of magnitude estimate would be that 1.2 metric tons of Mn (about 0.28  $\text{m}^3$  at 50% porosity) would be needed to produce 100 kg  $\text{NH}_3$  per day by chemical looping. Improvements by minimizing parasitic dinitrogen formation through better distributed Na promoter on the particles are certainly within reach so that the Mn amount estimated here could be seen as a worst case. To minimize gas phase

transport issues, the Mn could be deposited in a ceramic multi-channel monolith as industrially available for catalytic converters, for example.

#### 4. Summary and Outlook

In summary, the addition of NaOH as alkali-containing promoter significantly improves yield and kinetics of chemical looping of Mn for NH<sub>3</sub> synthesis at atmospheric pressure. The process uses earth-abundant materials at increased temperature. Reduced particle size and more evenly distributed promoter could likely improve yield and cycling time for a technical process. Dispersing the particles in a porous carrier such as a ceramic foam or porous ceramic monolith might address the issue of particle interaction at high temperatures. An order of magnitude estimate based on the results here would be that 100 kg NH<sub>3</sub> per day could be produced using about 1,200 kg of Mn in chemical looping with N<sub>2</sub> and H<sub>2</sub>.

#### Supporting Information

Supplementary information is available online.

#### Acknowledgments

This material is based upon work supported by the National Science Foundation under Grant No. 1856084 for the FEWtures project. Partial support by the U.S. Department of Energy, Office of Science, under Award Number DOE EPSCOR 0001572 for C. Huang is acknowledged. We gratefully acknowledge access to the Franceschi Microscopy and Imaging Center, L.J. Smith Hall, at Washington State University. The authors also would like to acknowledge Dr. Valerie Lynch-Holm, for her assistance in the imaging center.

## Symbols and Greek letters

T [°C] Temperature

t [min] Time

wt% Weight percent

Author Manuscript

## Table and Figure captions

**Figure 10:** Principle of chemical looping NH<sub>3</sub> synthesis from H<sub>2</sub> and N<sub>2</sub> at atmospheric pressure and elevated temperature. Mn nitrides are used as N carriers. Parasitic N<sub>2</sub> formation during NH<sub>3</sub> harvest lowers the yield (right side). Incomplete N removal during harvest creates a dead load. (Atomic diameters roughly to scale; a simplified Mn lattice is shown).

**Figure 11.** Overall process and parameters of chemical looping tests in "stop mode" reported here. m, w, i, and e indicate weighing, WAXD, I.C.P., and S.E.M., respectively. "air" indicates that the cooled sample was removed from the furnace, manually ground with mortar and pestle, and returned to the furnace.

**Figure 12.** Scanning electron micrograph of as-received Mn particles. The size distribution is significant with a population of larger particles (on the order of 10 μm), and a population with a much smaller size (on the order of 1-8 μm).

**Figure 13.** System for chemical looping. (1) N<sub>2</sub> cylinder, (2) H<sub>2</sub> cylinder, (3) metering valve, (4) pressure gauge, (5) mass flow controller, (6) fused quartz furnace tube, (7) electric tube furnace, (8) alumina combustion boat with solid reactant, (9) tube end cap, (10) gas washbottle, (11), (12) Dräger NH<sub>3</sub> gas detection tube sampling, and (13) bubble flowmeter.

**Figure 14.** Ammonia harvest from the first chemical looping cycle of about 5 grams of Mn, and 5 grams Mn with 0.25 grams NaOH promoter added in both stop mode (solid symbols) and non-stop mode (open symbols). Two subsequent nitridation/harvest cycles were performed but are essentially identical and omitted here (see supporting information for all three looping cycles of Mn and Mn with promoter). The addition of Na promoter and non-stop mode significantly improves yield and cycle time.

**Figure 15.** Side-by-side comparison for WAXD spectra of the solid after initial nitridation and after final NH<sub>3</sub> harvest during chemical looping with and without NaOH promoter. The similarity of the spectra and their expected change upon nitridation (prominent nitride peaks indicated by solid square, and triangle: Mn<sub>2</sub>N<sub>0.86</sub> (PDF number: 01-077-2007) and Mn<sub>4</sub>N (PDF number: 01-089-7380), respectively) supports the notion that the promoter does not impact the bulk of the solid, but modifies the conversion of N with H<sub>2</sub> to NH<sub>3</sub> at the solid surface (additional peak assignments can be found in the on-line materials).

**Figure 16.** Wide-angle x-ray diffraction patterns of (a) as received Mn, (b1),(b2) and (b3) Mn after first, second, and third nitridation, respectively. Solid circle, square, and triangle: MnO (Powder Diffraction File (PDF) number: 01-077-2929), Mn<sub>2</sub>N<sub>0.86</sub> (PDF number: 01-077-2007) and Mn<sub>4</sub>N (PDF number: 01-089-7380), respectively (additional peak assignments can be found in the on-line materials ).

**Figure 17.** XPS Mn<sub>2p3/2</sub> spectra for as-received Mn particles. The surface appears to contain only oxides, and metallic Mn is considered below the detection limit.

**Figure 18.** WAXD spectra of Mn nitride before (a) and after (b) NH<sub>3</sub> harvesting. Some nitride remains after NH<sub>3</sub> harvesting levels off likely due to increasing N diffusion limitations in the solid particles as the outermost nitride is depleted first. Solid circle, square, and triangle: MnO (PDF number: 01-077-2929), Mn<sub>2</sub>N<sub>0.86</sub> (PDF number: 01-077-2007) and Mn<sub>4</sub>N (PDF number: 01-089-7380), respectively, and also the hollow circle shows Mn (PDF number: 01-089-2412).

## References:

- [1] P. H. Pfromm, *J. Renew. Sustain. Energy* **2017**, 9(3), 034702. doi:10.1063/1.4985090
- [2] S. Giddey, S. P. S. Badwal, C. Munnings, M. Dolan, *ACS Sustainable Chem. Eng.* **2017**, 5, 10231-10239. doi:10.1021/acssuschemeng.7b02219
- [3] [www.iea.org/reports/the-future-of-hydrogen](http://www.iea.org/reports/the-future-of-hydrogen) (Accessed on June 01, 2019)
- [4] M. Apple, Wiley Online Libr. **2006**. doi.org/10.1002/14356007.a02\_143.pub2
- [5] J. R. Jennings, *Catalytic Ammonia synthesis, fundamentals and practice*, Plenum Press New York (NY) **1991**.
- [6] [www.peninsuladailynews.com](http://www.peninsuladailynews.com) (Accessed on February 28, 2019)
- [7] [www.ageconsearch.umn.edu/record/133410](http://www.ageconsearch.umn.edu/record/133410) (Accessed on September 01, 2019)
- [8] [www.turbomachinery.man-es.com/applications/downstream/ammonia-urea](http://www.turbomachinery.man-es.com/applications/downstream/ammonia-urea) (Accessed on February 01, 2019)
- [9] R. Michalsky, P. H. Pfromm, *J. Sol. Energy* **2011**, 85(11), 2642-2654. doi:10.1016/j.solener.2011.08.005
- [10] R. Michalsky, B. J. Parman, V. Amanor-Boadu, P. H. Pfromm, *Energy* **2012**, 42(1), 251-260. doi:10.1016/j.energy.2012.03.062
- [11] L. Kyle, R. Crooks, M. Y. Darensbourg, L. Seefeldt, P. King, P. Holland, K. Bren, B. Hoffman, R. Schrock, M. Janik, A. Jones, M. Bullock, M. Kanatzidis, J. Chen, S. Lyman, P. H. Pfromm, W. Schneider, *Science* **2018**, 360(873). doi:10.1126/science.aar6611
- [12] L. Fan, L. Zeng, S. Luo, *AIChE J.* **2015**, 61(1), 2-22. doi:10.1002/aic.14695
- [13] R. Michalsky, P. H. Pfromm, *J. Phys. Chem. C* **2012**, 116(44), 23243-2325. doi:10.1021/jp307382r
- [14] R. Michalsky, P. H. Pfromm, US Patent 10,315,967, **2019**.
- [15] M. Ayiania, F. M. Cabajal-Gamarra, T. Garcia-Perez, C. Frear, W. Suliman, M. Garcia-Perez, *Biomass Bioenergy* **2019**, 120, 339-349. doi:10.1016/j.biombioe.2018.11.028
- [16] D. Hobbs, J. Hafner, D. Spisak, *Phys. Rev. B.* **2003**, 68(1), 014407. doi:10.1103/PhysRevB.68.014407
- [17] A. Miura, C. Rosero-Navarro, Y. Msubuchi, M. Higuchi, S. Kikkawa, K. Tadanaga, *Angew. Chem.* **2016**, 55(28), 7963-7967. doi:10.1002/anie.201601568
- [18] M. Heidlage, E. A. Kezar, K. Snow, P. H. Pfromm. *Ind. Eng. Chem. Res.* **2017**, 56(47), 14014-14024. doi:10.1021/acs.iecr.7b03173

- [19] R. C. Weast, Handbook of Chemistry and Physics, C.R.C. Press, West Palm Beach (FL) **1977-1978**
- [20] A. Bayon, V. A. de l Pena O'Shea, D. P. Serrano, J. M. Coronado, Int. J. Hydrog. Energy **2013**, 38(30), 13143-13152. doi:10.1016/j.ijhydene.2013.07.101
- [21] B. Xu, B. Yashodhan, M. E. Davis, PNAS. **2012**, 109(24), 9260-9264. doi:10.1073/pnas.1206407109
- [22] D. D. Williams, J. A. Grand, R. R. Miller, J. Am. Chem. Soc. **1956**, 78(20), 5150 – 5155. doi:10.1021/ja01601a004

Author Manuscript

## Entry for the Table of Contents

Chemical looping in the presence of Na as a promoter boosted the ammonia harvesting. Based on the feasible reactions on the Mn surface, Na may increase the N conversion to  $\text{NH}_3$  instead of  $\text{N}_2$  whereas, the reproducibility of successive reproducible looping implies unflinching.

